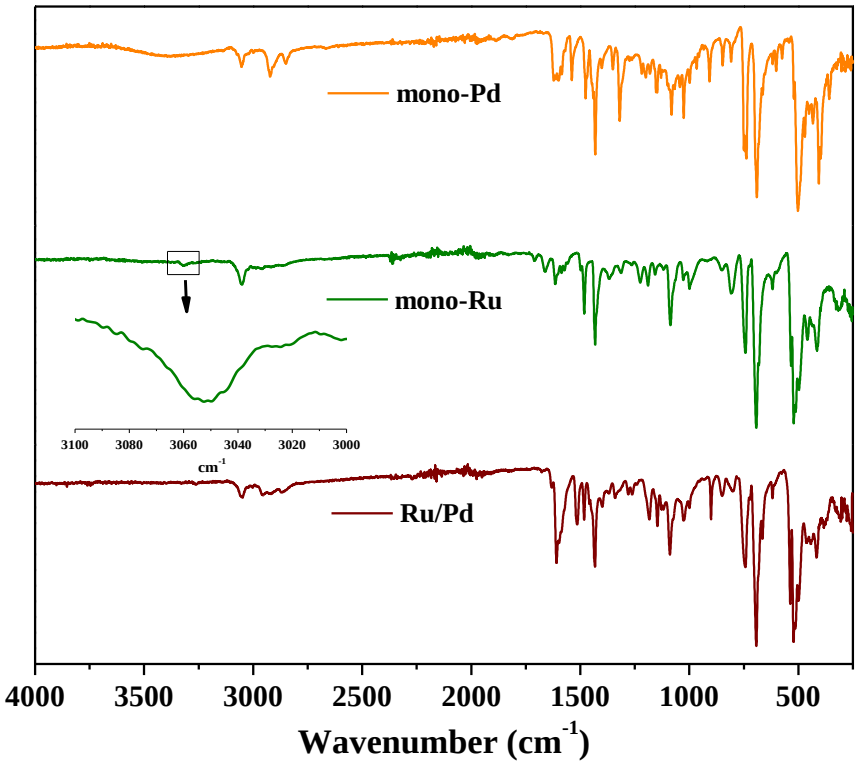

Figure S1. FTIR spectra of complexes mono-Pd, mono-Ru and Ru/Pd.

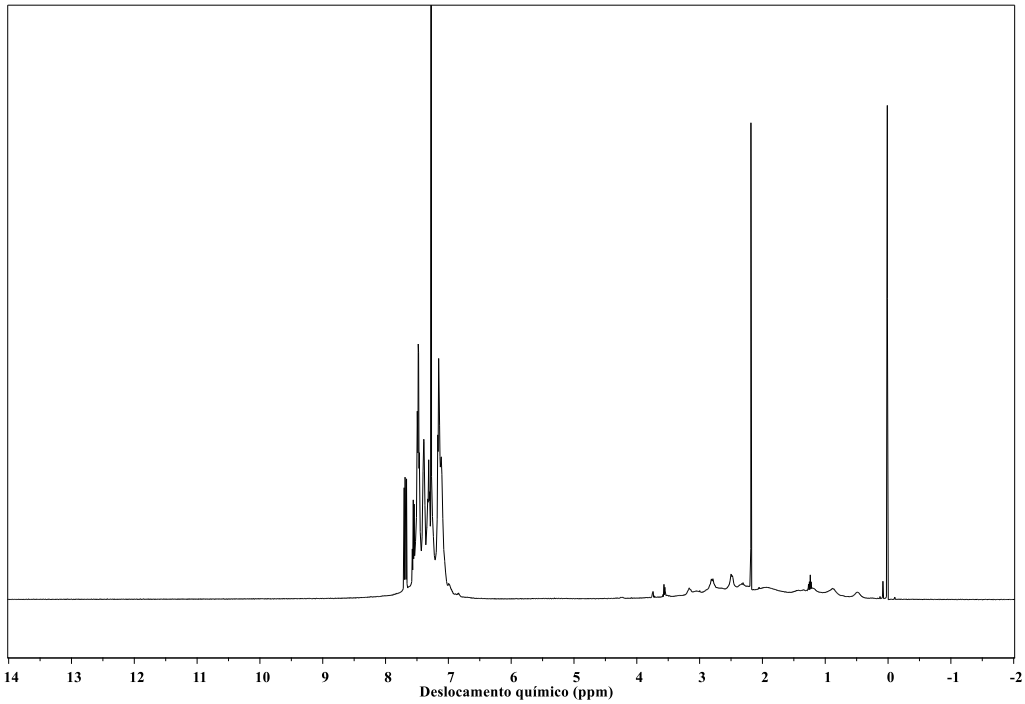

Figure S2. ^{1}H NMR spectrum of mono-Ru in $CDCl_3$.

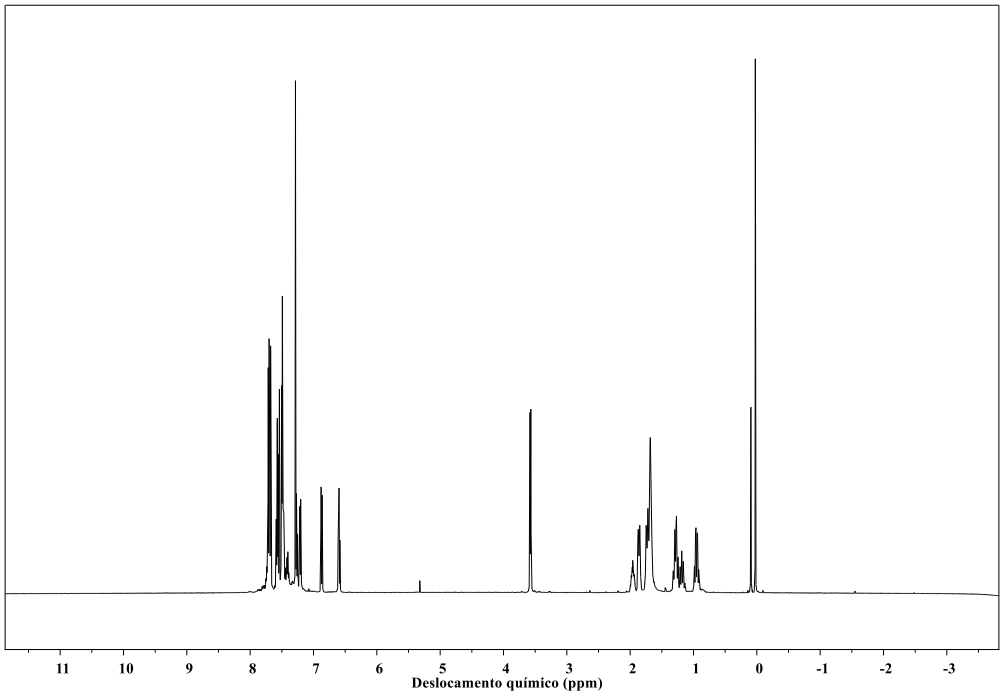

Figure S3. ^{1}H NMR spectrum of mono-Pd in $CDCl_3$.

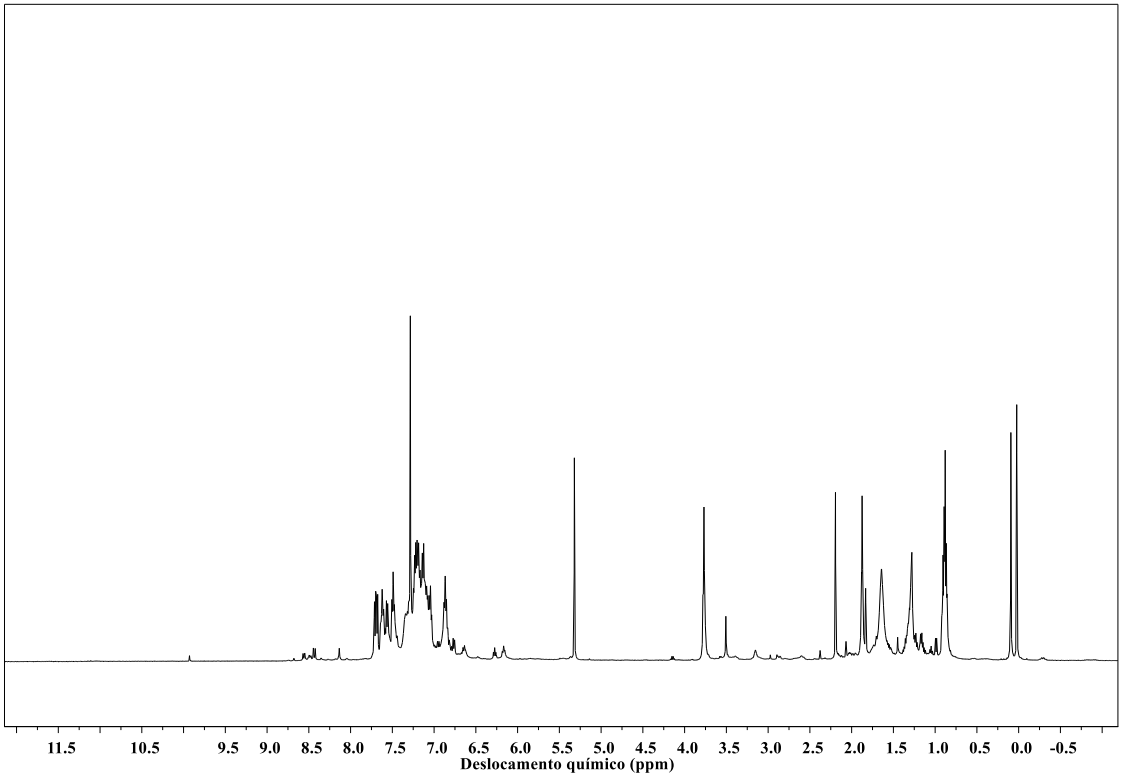

Figure S4. ^{1}H NMR spectrum of Ru/Pd in $CDCl_3$.

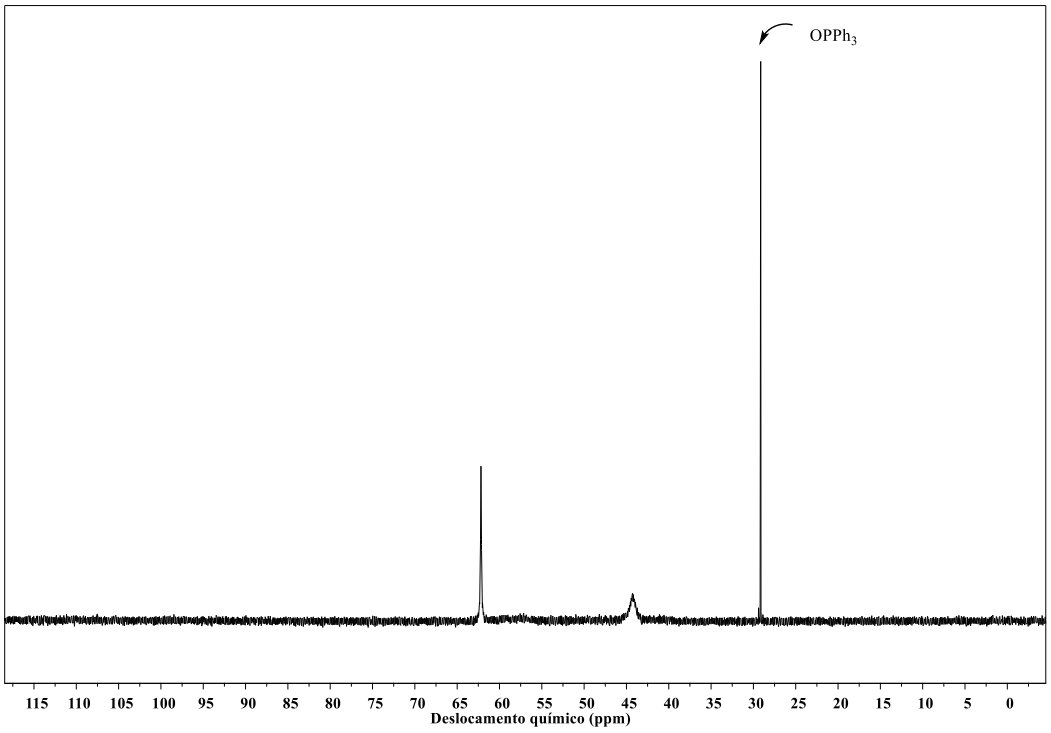

Figure S5. $^{31}P\{^{1}H\}$ NMR spectrum of mono-Ru in $CDCl_3$.

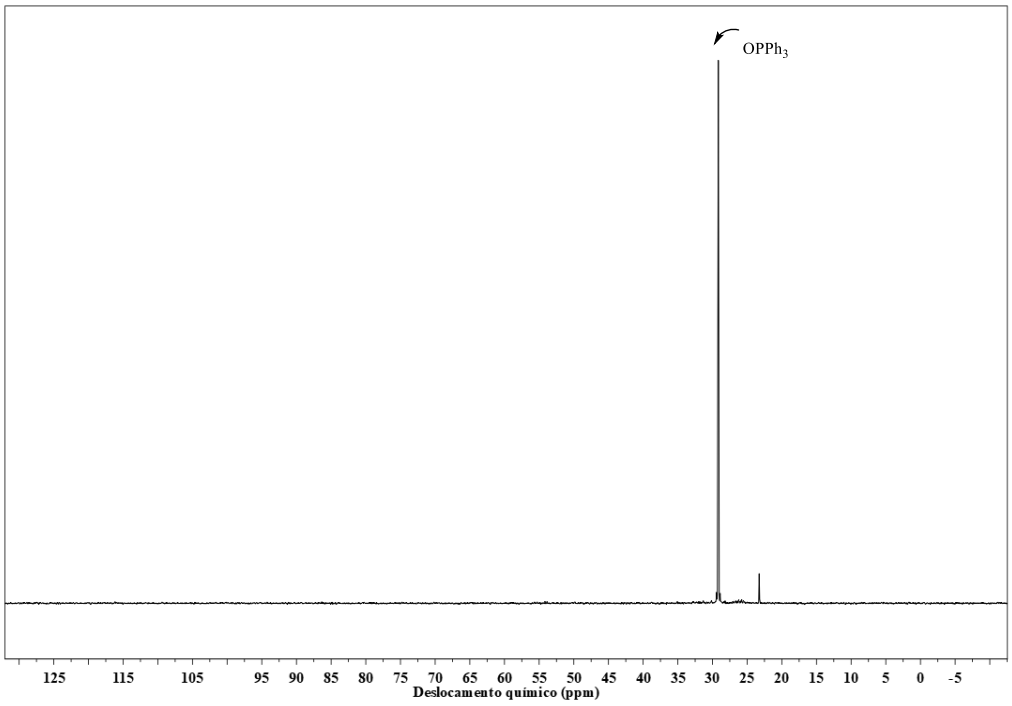

Figure S6. $^{31}P\{^{1}H\}$ NMR spectrum of mono-Pd in $CDCl_3$.

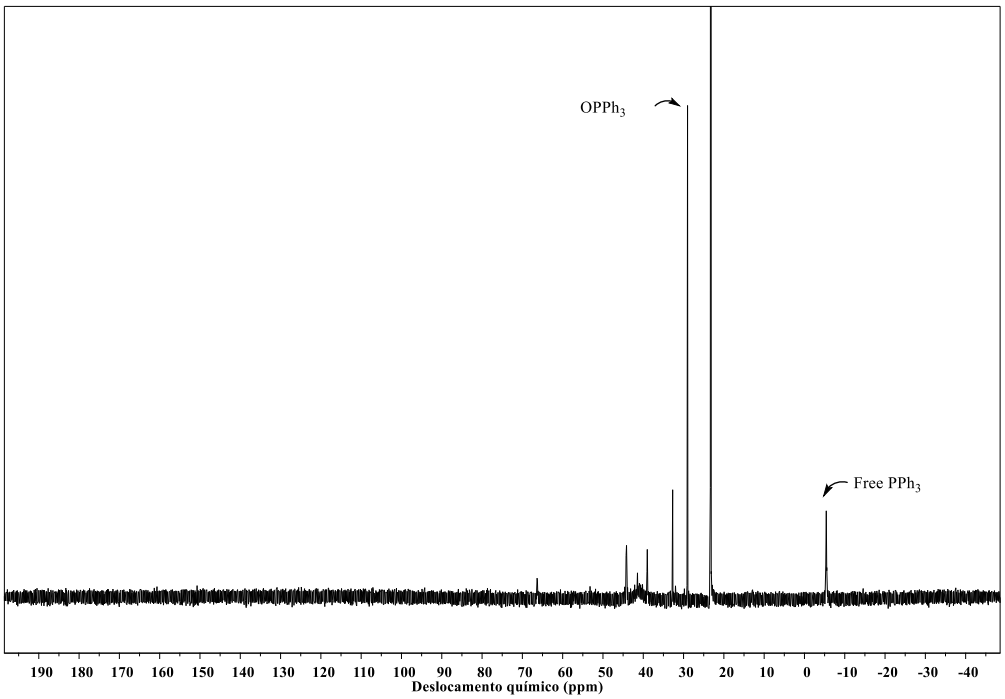

Figure S7. $^{31}P\{^{1}H\}$ NMR spectrum of mono-Ru in $CDCl_3$.

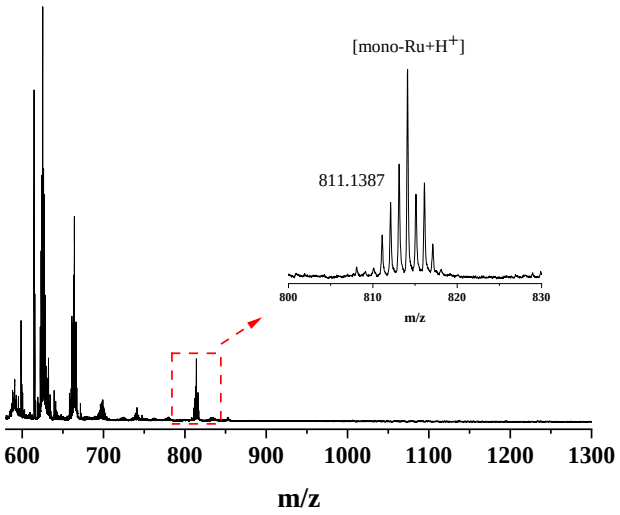

Figure S8. MALDI-TOF spectroscopy of mono-Ru from CH_2Cl_2 solution. Matrix: α-cyano-4-hydroxycinnamic acid.

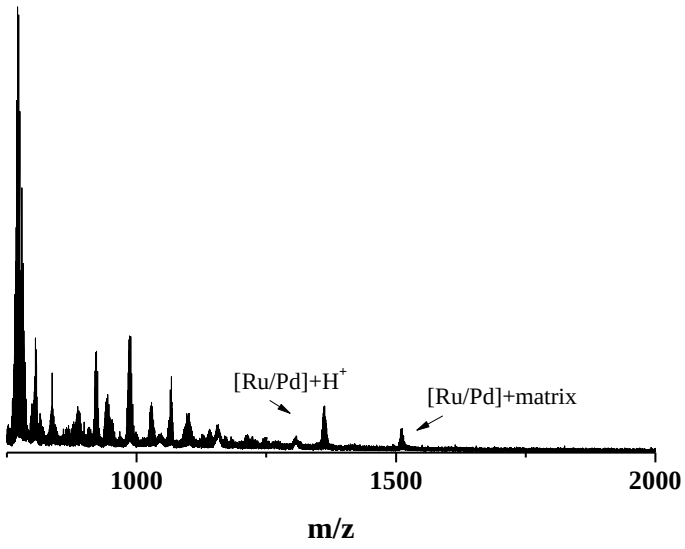

Figure S9. MALDI-TOF spectroscopy of Ru/Pd from CH_2Cl_2 solution. Matrix: α-cyano-4-hydroxycinnamic acid.

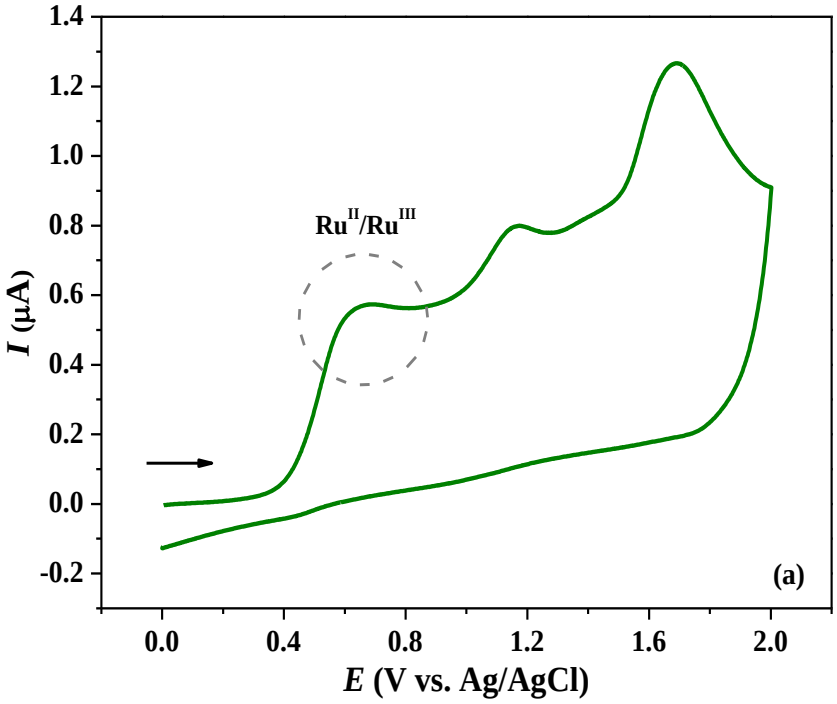

Figure S10. Cyclic voltammograms of mono-Ru from CH_2Cl_2 solutions at 25 ºC. Scanning anodically from 1.0 to 2.0 V at scan rate of 100 mV s^{-1}. [mono-Ru] = 1.0 mmol L^{-1}; [*n*-Bu_4NPF_6] = 0.1 mol L^{-1}.

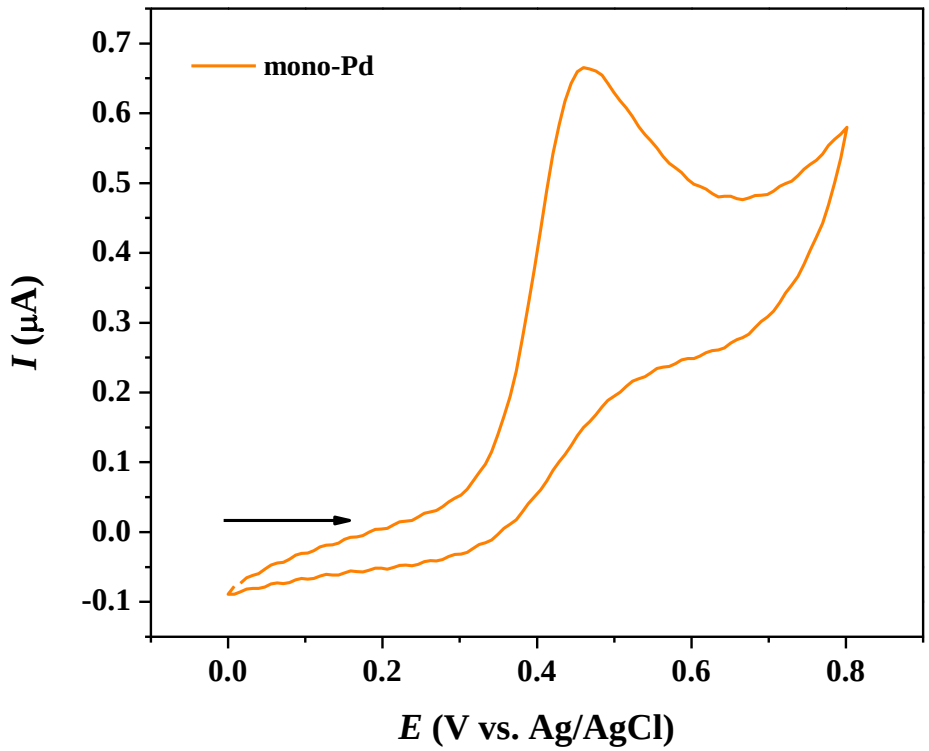

Figure S11. Cyclic voltammograms of mono-Pd from CH_2Cl_2 solutions at 25 ºC. Scanning anodically from 0.0 to 0.8 V at scan rate of 100 mV s^{-1}. [mono-Pd] = 1.0 mmol L^{-1}; [*n*-Bu_4NPF_6] = 0.1 mol L^{-1}.

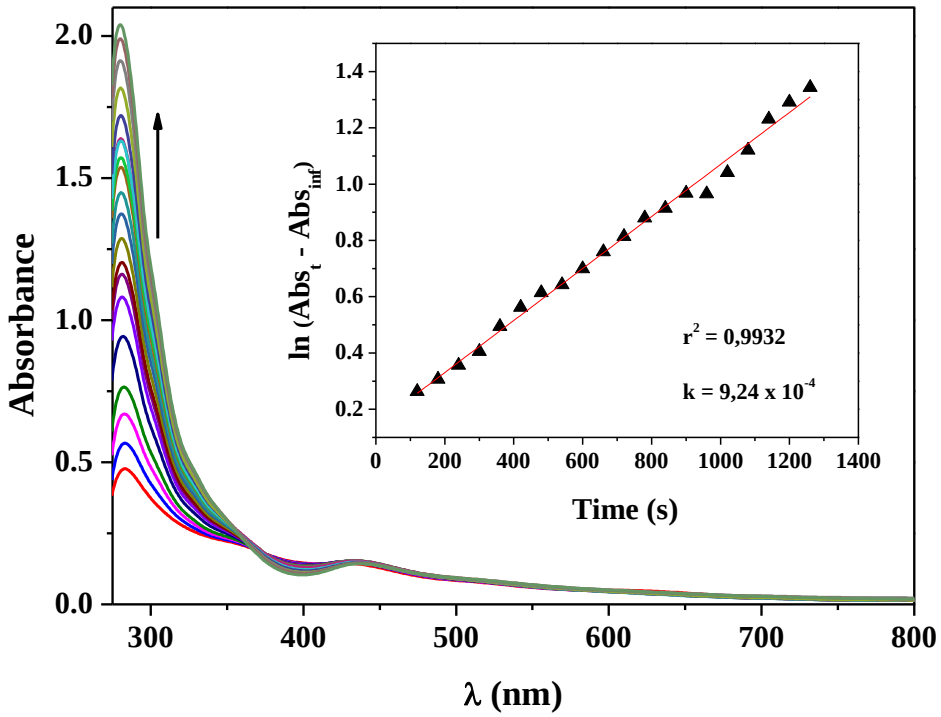

Figure S12. Kinetic study of mono-Ru in presence of EDA monitored by electronic spectroscopy every 30 seconds and (*insert*) dependence of ln(Abs_t -Abs_{inf}) as a function of time at 316 nm. [Ru] = 1.0 × 10^{-5} mol L^{-1}; [EDA] = 1.26 × 10^{-5} mol L^{-1} in CH_2Cl_2 and 25 ºC.

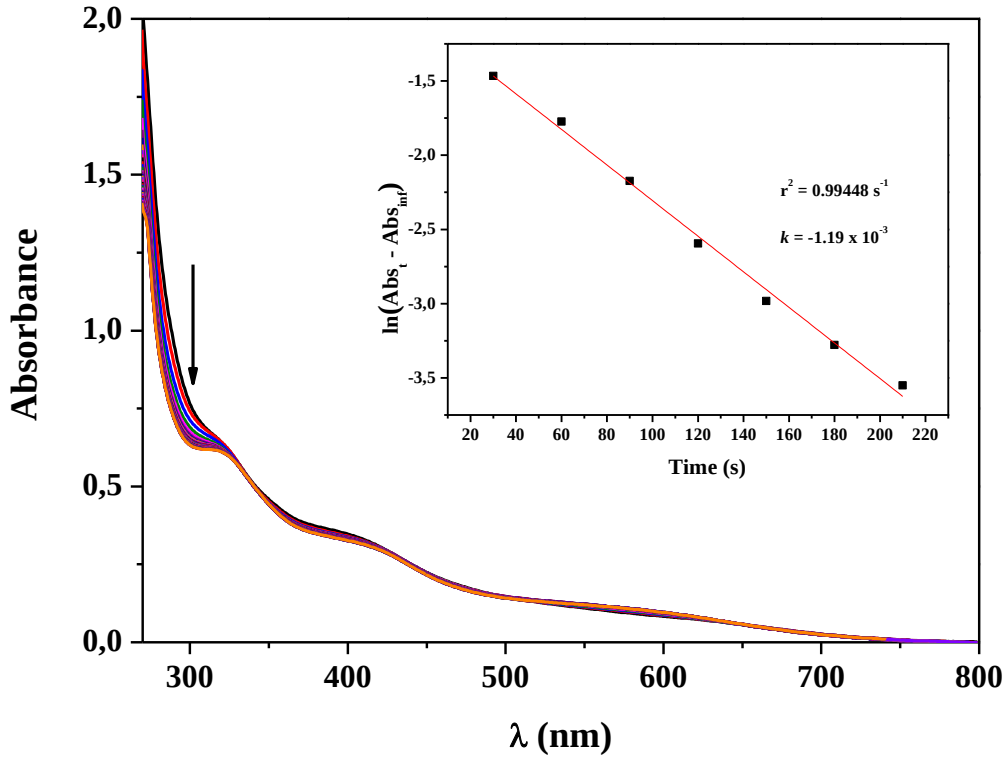

Figure S13. Kinetic study of Ru/Pd in presence of EDA monitored by electronic spectroscopy every 30 seconds and (*insert*) dependence of $\ln(Abs_t - Abs_{inf})$ as a function of time at 297 nm. [Ru] = 1.0×10^{-5} mol L^{-1}; [EDA] = 1.26×10^{-5} mol L^{-1} in CH_2Cl_2 and 25 ºC.